OMTN, Volume *23*

Supplemental Information

Association of clock-like mutational signature with immune checkpoint inhibitor outcome in patients with melanoma and NSCLC

Wei Chong, Zhe Wang, Liang Shang, Shengtao Jia, Jin Liu, Zhen Fang, Fengying Du, Hao Wu, Yang Liu, Yang Chen, and Hao Chen

Supplementary information

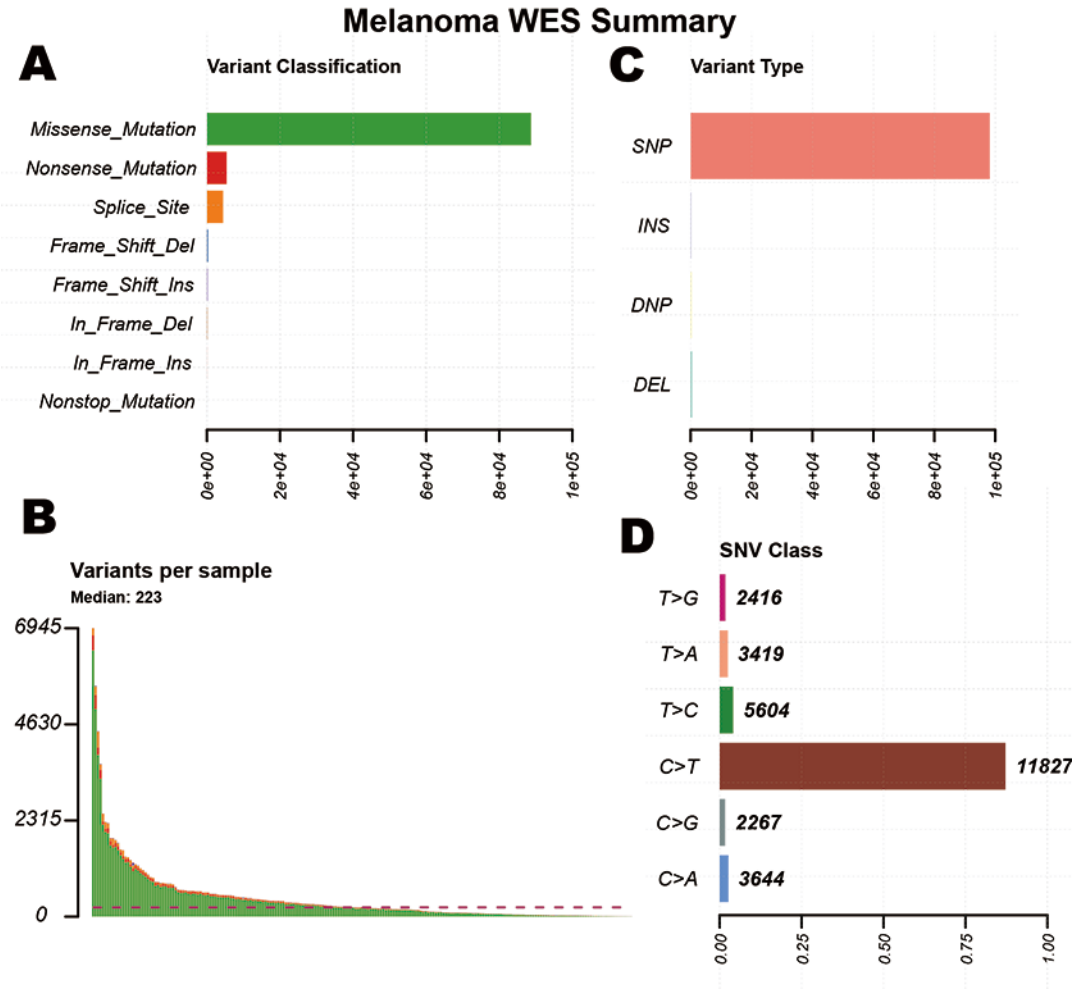

Figure S1. Characteristics of the mutational counts and proportion in the melanoma genomic mutational profile. Bar-plot representation of the variant classification(A), variant counts(B), variant type(C) and six bases substitution type (D) of the melanoma genomic data.

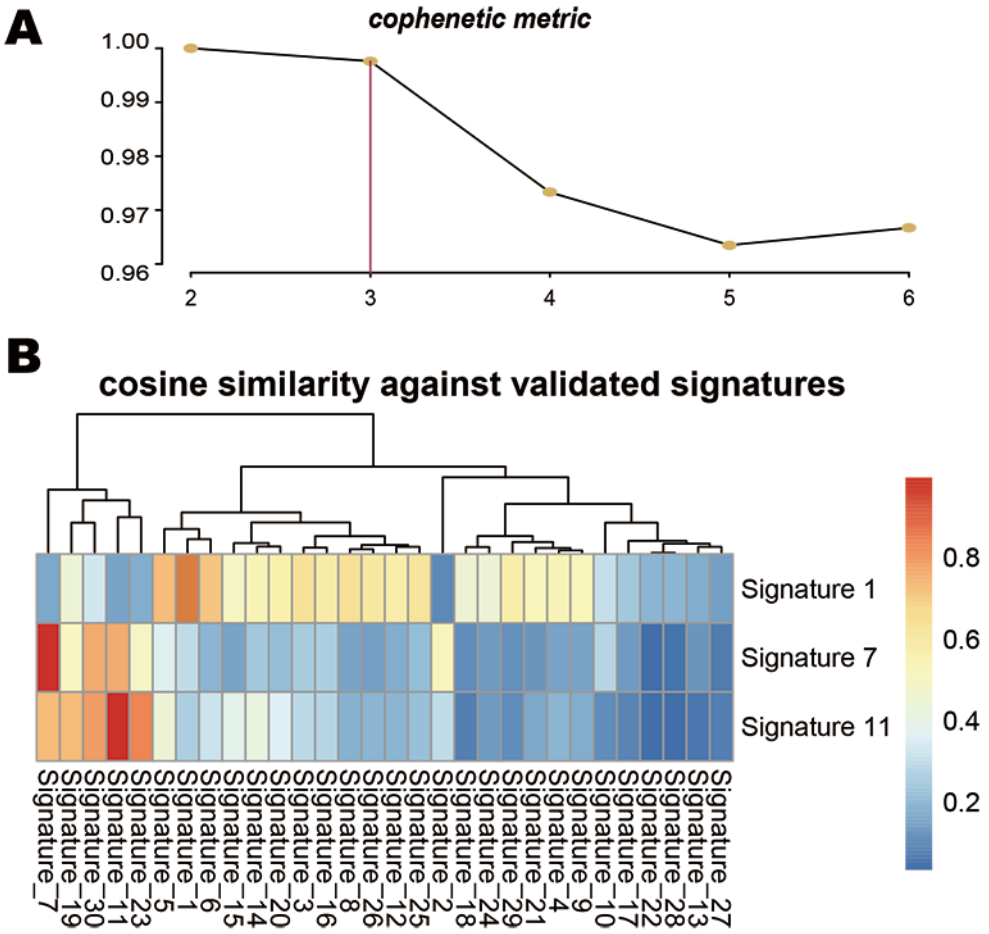

Figure S2. Mutational signatures extracted from the aggregated melanoma dataset.

(A) The progress of automatically determines the optimal number of mutational signatures (n=3). (B) Cosine similarity analysis of extracted mutational signatures against the 30 identified signatures in Catalogue of Somatic Mutations in Cancer (COSMIC, v2) with heatmap illustration.

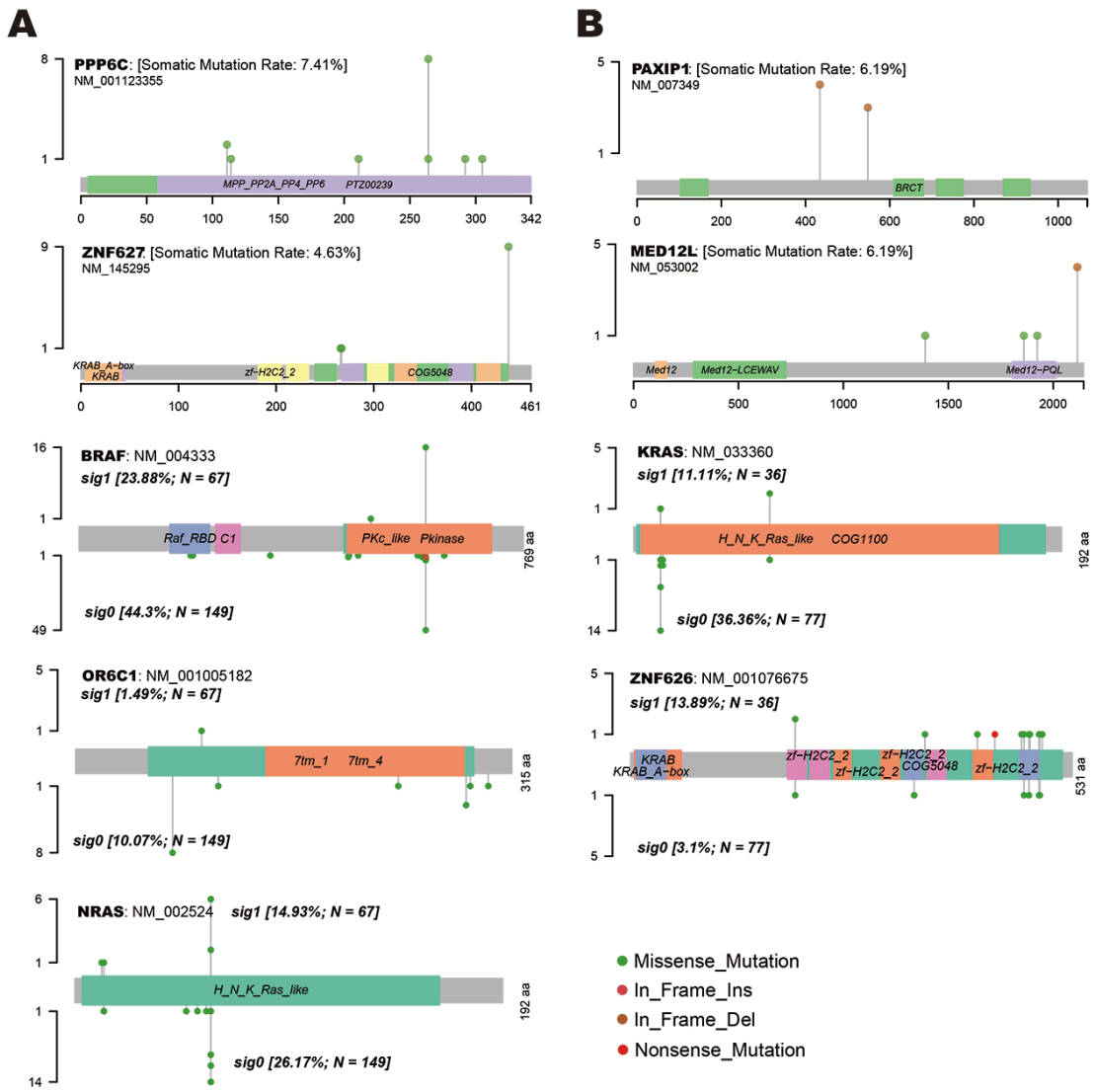

Figure S3. Lollipop plot showed the mutation distribution (different color) and functional domains of cancer driver genes in melanoma (A) and NSCLC (B) cohort.

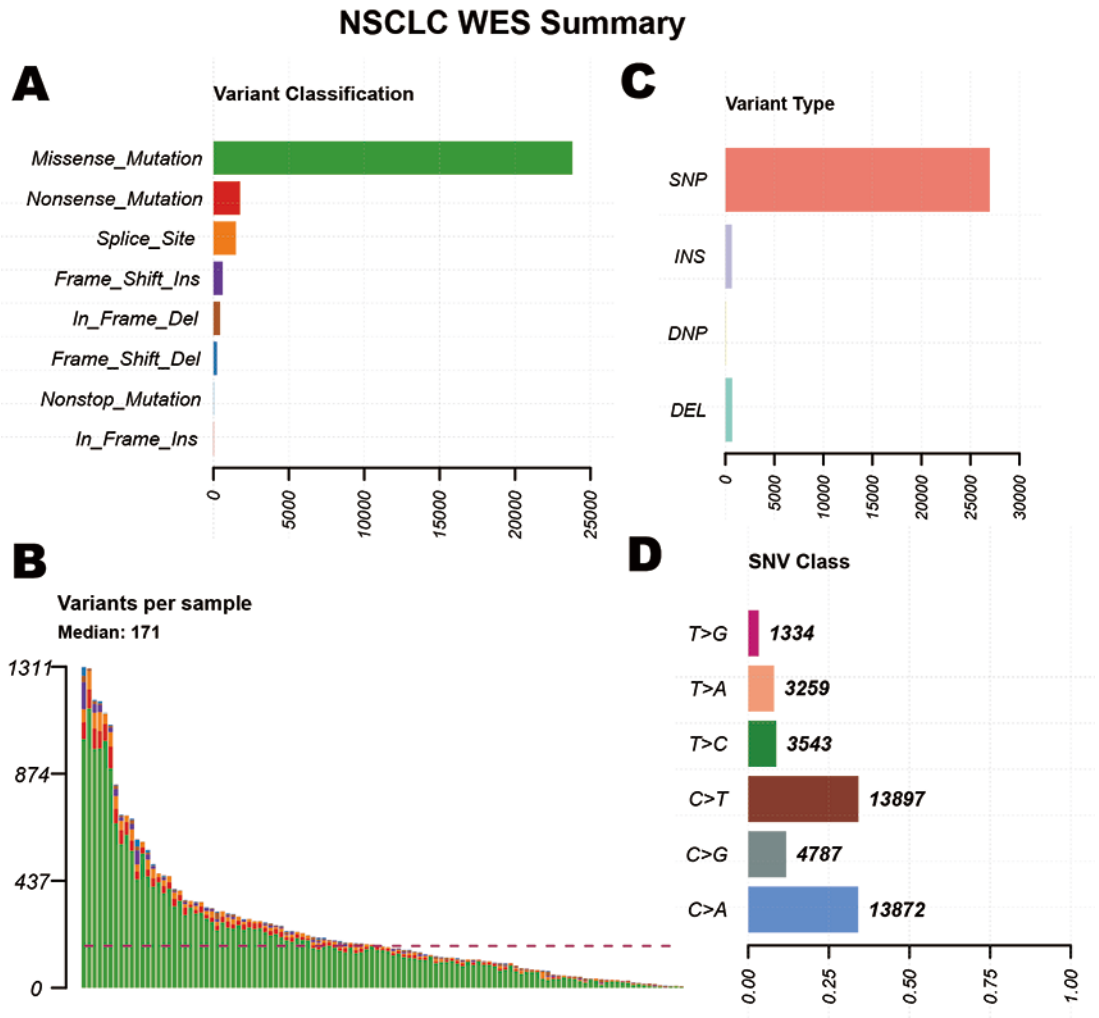

Figure S4. Characteristics of the mutational counts and proportion in the aggregated NSCLC genomic mutational profile. Bar-plot representation of the variant classification(A), variant counts(B), variant type(C) and six base substitution type (D) of the NSCLC genomic data.

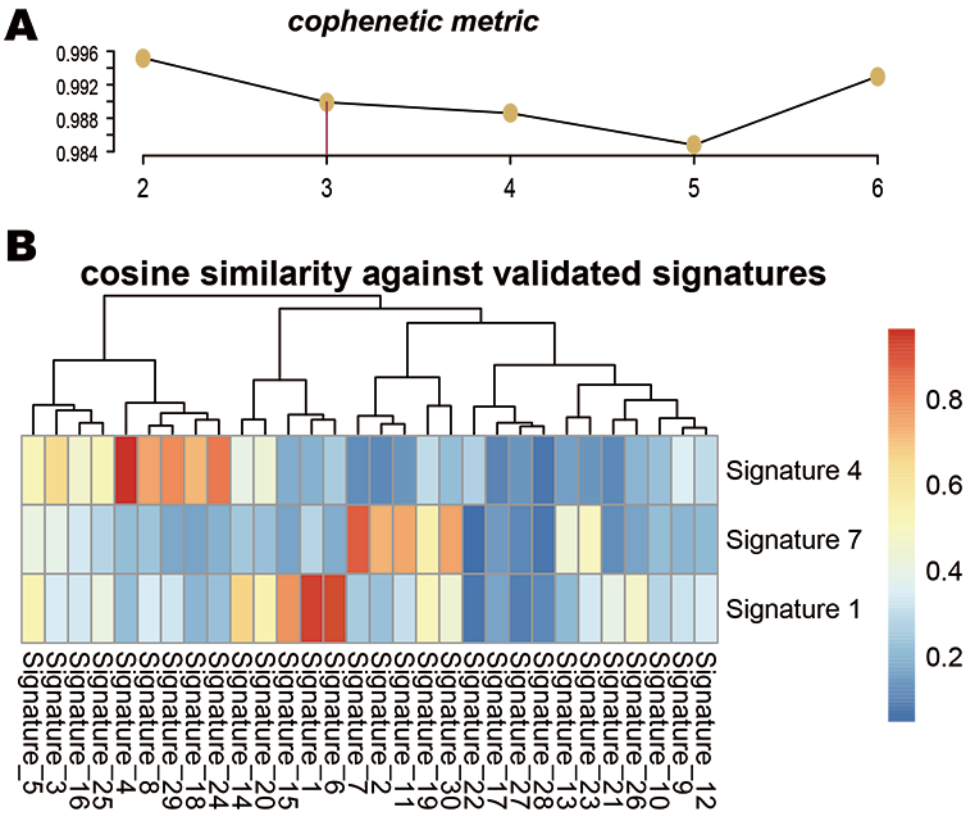

Figure S5. Mutational signatures extracted from the aggregated NSCLC dataset. (A) The progress of automatically determines the optimal number of mutational signatures (n=3). (B) Cosine similarity analysis of extracted mutational signatures against the 30 identified signatures in Catalogue of Somatic Mutations in Cancer (COSMIC, v2) with heatmap illustration.

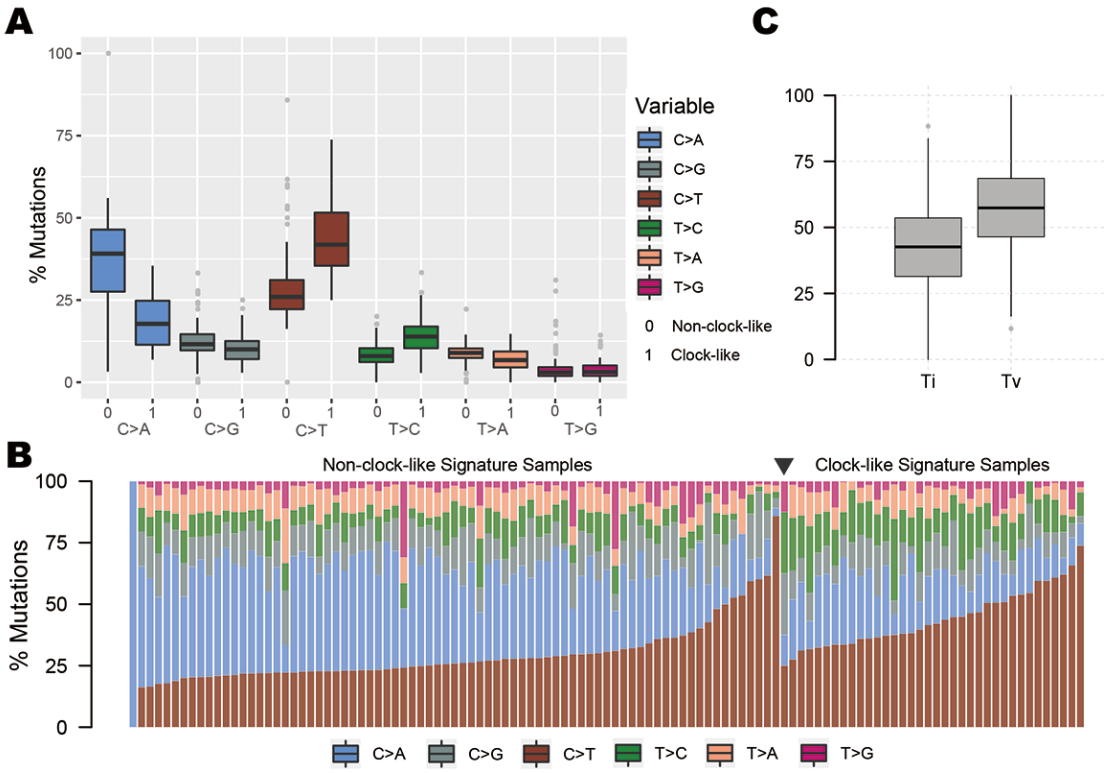

Figure S6. Mutational counts and proportion of the six bases substitution type in each of the NSCLC samples. Representation of boxplot (A) and bar plot (B) of the six bases substitution type (C>A, C>G, C>T, T>C, T>A, T>G), which classified by the clock-like signature status. (C) The frequency of transition vs transversion mutations in NSCLC.

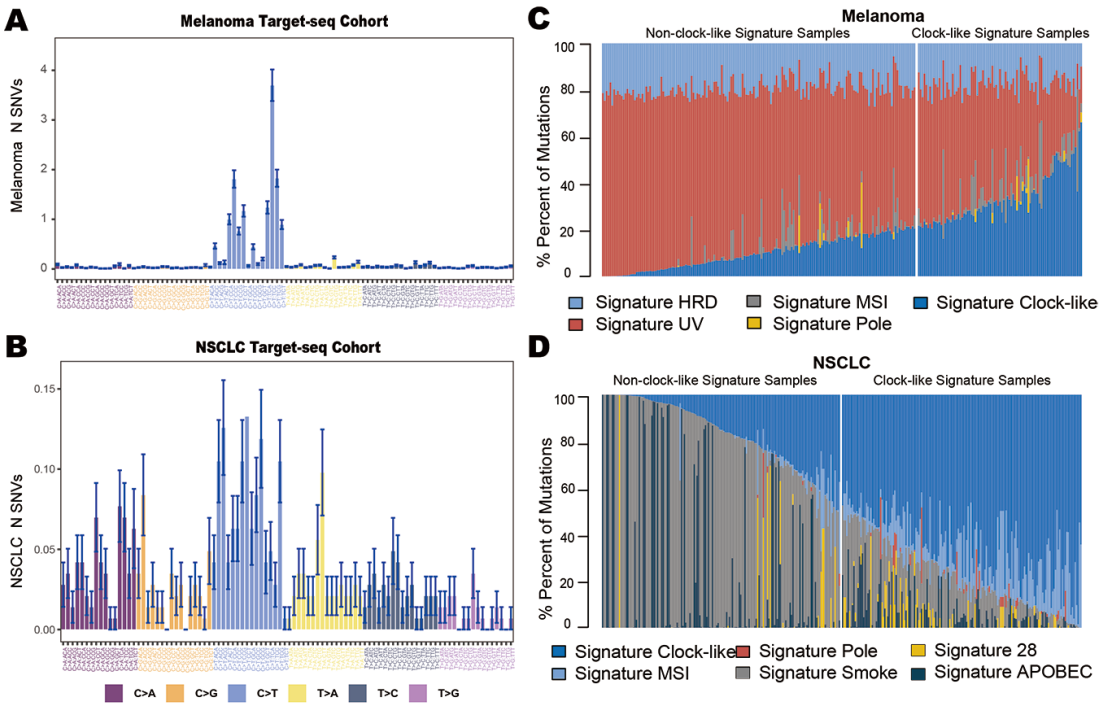

Figure S7. Mutational signatures extracted from the targeted-NGS panels datasets with the SigMA analysis tool. The 96 mutational contexts (i.e., C > A, C > G, C > T, T > A, T > C, T > G, and their 5' and 3'' adjacent bases) extracted from the melanoma (A) and NSCLC (B) targeted NGS-panel (MSK-IMPACT) datasets. Mutational exposures (number of mutations) were attributed to extracted mutation signatures in each of melanoma (C) and NSCLC (D) samples.

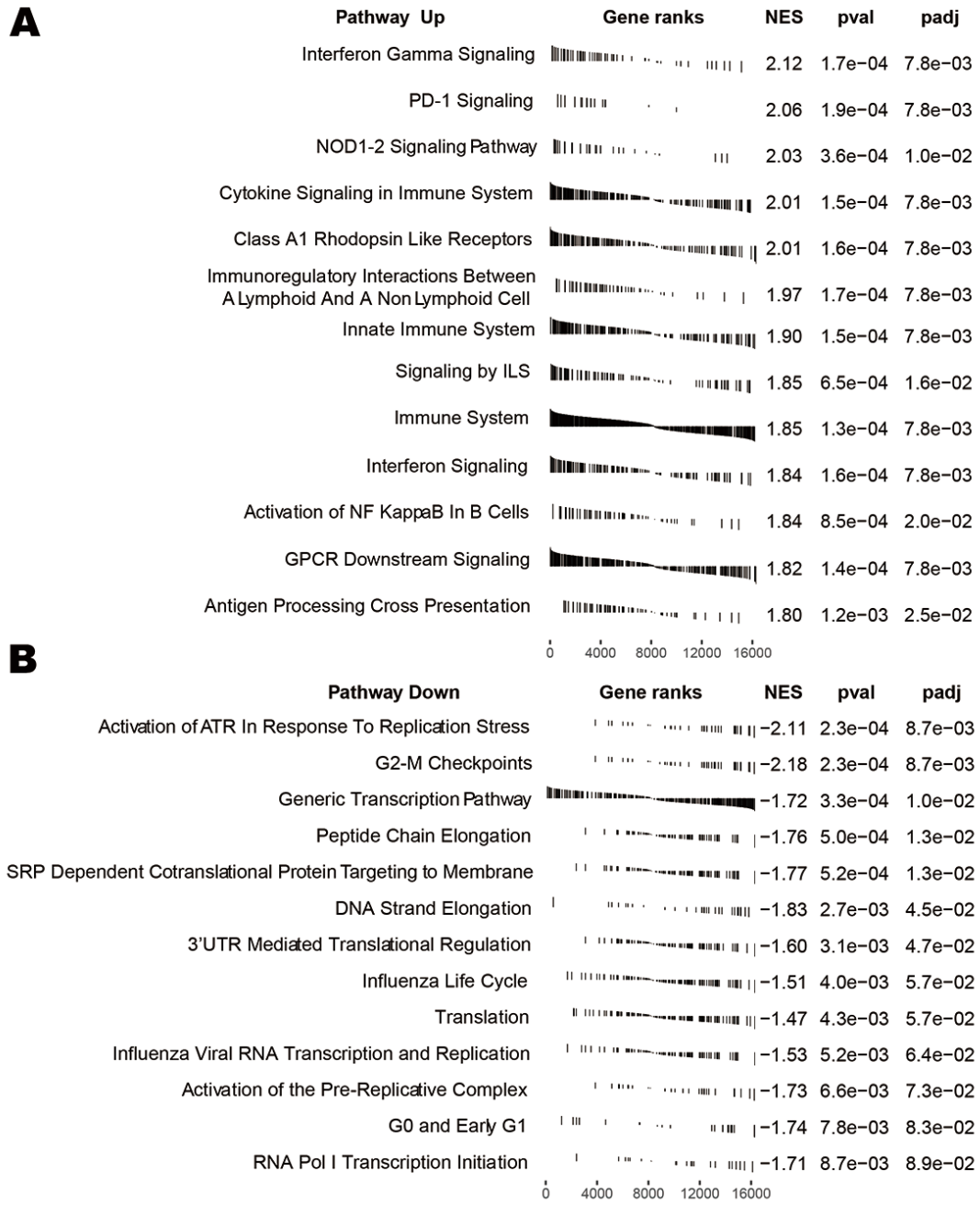

Figure S8. GSEA enrichment plots shown enriched gene sets against to REACTOME datasets in non-clock-like vs clock-like groups. (A) Up-regulated pathways and (B) Down-regulated pathways. NES, Normalized Enrichment Score.

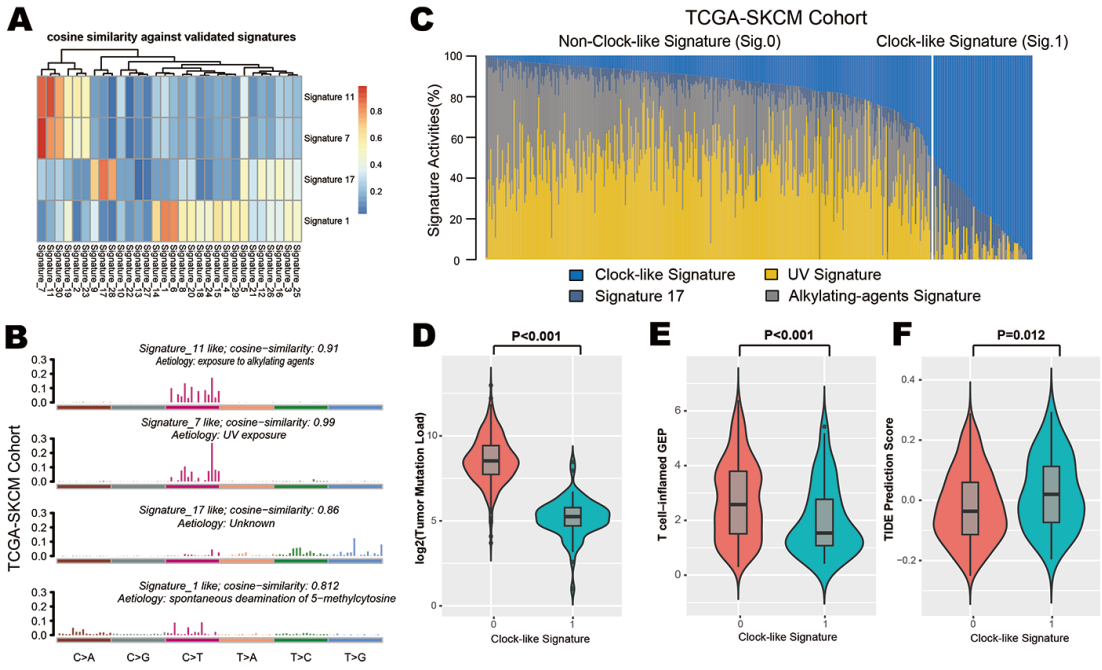

Figure S9. The extracted mutational signatures from the TCGA skin cutaneous melanoma (SKCM) datasets. (A) Cosine similarity analysis of extracted mutational signatures against the 30 identified signatures in Catalogue of Somatic Mutations in Cancer (COSMIC, v2) with heatmap illustration. (B) Mutational exposures (number of mutations) were attributed to extracted mutation signatures in SKCM samples. (C) The mutational activities of corresponding extracted mutational signatures (UV signature, alkylating-agents signature, clock-like signature and signature 17). (D) Tumor mutation load was evaluated and compared in different clock-like mutation signature grouping. (E) Distribution and association of T cell-inflamed GEP score in clock-like versus non-clock-like signature subgroup. (F) Distribution of TIDE immune resistance prediction scores in TCGA-SKCM cohort stratified by clock-like signature grouping.

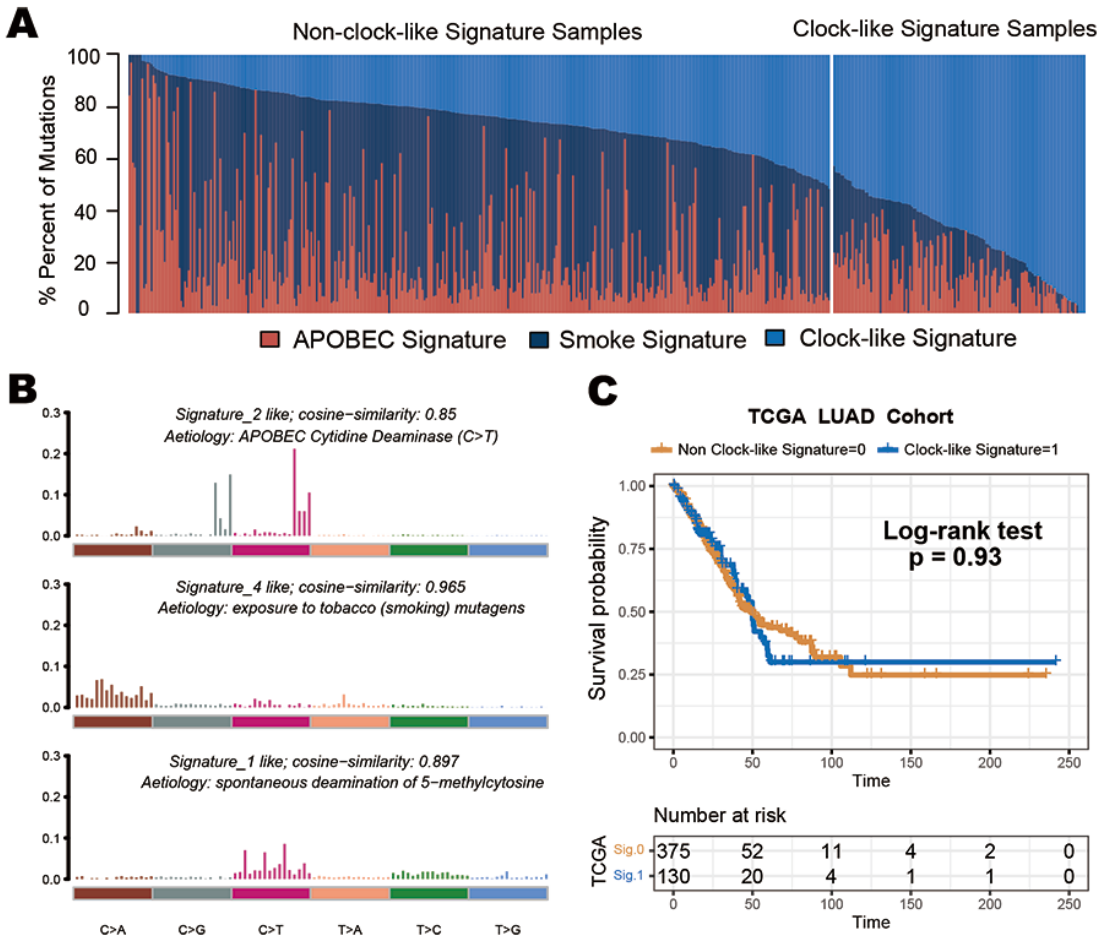

Figure S10. The extracted mutational signatures from the TCGA lung adenocarcinoma(LUAD) datasets. (A) Mutational exposures (number of mutations) were attributed to extracted mutation signatures in LUAD samples. (B) The mutational activities of corresponding extracted mutational signatures (APOBEC signature, smoke signature and clock-like signature, named as COSMIC signature). The trinucleotide base mutation types were on the X-axes, whereas Y-axes showed the percentage of mutations in the signature attributed to each mutation type. (C) Kaplan-Meier survival analysis classified by clock-like mutation signature grouping.

Table S1. Detailed clinical characteristics of 216 WES samples in melanoma.

Table S2. Detailed clinical characteristics of 113 WES samples in NSCLC.

Table S3. Detailed clinical characteristics of 253 targeted-sequencing samples in melanoma.

Table S4. Detailed clinical characteristics of 339 targeted-sequencing samples in NSCLC.

Table S5. Detailed clinical characteristics and mutational signatures of 451 SKCM samples from TCGA.

Table S6. Detailed clinical characteristics and mutational signatures of 514 LUAD samples from TCGA.